Journal of Radiotherapy in Practice

cambridge.org/jrp

Original Article

Cite this article: Kongsa A, Chitapanarux I, Watcharawipha A, Huntrakul L, Thongsuk W, and Klunklin P. (2023) Improvement of matching fields using coplanar field border method in postmastectomy radiotherapy. *Journal of Radiotherapy in Practice*. **22**(e8), 1–8. doi: 10.1017/S1460396921000431

Received: 3 April 2021
Revised: 3 June 2021
Accepted: 29 June 2021

Key words:
coplanar; half beam block; postmastectomy; three-dimensional radiotherapy

Author for correspondence:
Prof. Imjai Chitapanarux, MD, Division of Radiation Oncology, Department of Radiology, Faculty of Medicine, Chiang Mai University, 110 Intavaroros Rd., Sriphum, Chiang Mai, 50200, Thailand. Tel: +66-53-935456. Fax: +66-53-935491.
E-mails: imjai@cmu.ac.th, imjai@hotmail.com

Improvement of matching fields using coplanar field border method in postmastectomy radiotherapy

Anupong Kongsa[1,2], Imjai Chitapanarux[2,3,4], Anirut Watcharawipha[2,3], Lalita Huntrakul[5], Warit Thongsuk[2] and Pitchayaponne Klunklin[2,3]

[1]Graduate School, Chiang Mai University, Chiang Mai, Thailand; [2]Division of Radiation Oncology, Department of Radiology, Faculty of Medicine, Chiang Mai University, Chiang Mai, Thailand; [3]Northern Thai Research Group of Radiation Oncology (NTRG-RO), Faculty of Medicine, Chiang Mai University, Chiang Mai, Thailand; [4]Chiang Mai Cancer Registry, Faculty of Medicine, Maharaj Nakorn Chiang Mai Hospital, Chiang Mai University, Chiang Mai, Thailand and [5]Department of Radiology, Faculty of Medicine, Chiang Mai University, Chiang Mai, Thailand

Abstract

Aim: To propose a new matching method for the supraclavicular (SC) and tangential fields on three-dimensional radiotherapy (3DRT) for postmastectomy radiotherapy (PMRT).
Methods: A method of matching coplanar field borders (CFB) between the tangential and SC fields was created in 3DRT. The collimator angle of the medial tangential field was calculated to coplanar the SC field. The proposed method performance was ultimately benchmarked using the half beam block (HBB) and traditional three-field monoisocenter (TTM) methods by dosimetric comparison. The decision score was then employed to clarify the performance among these methods.
Results: The results show that the TTM method exhibited not only low doses on the organs at risk (OAR) but also on the matching fields. The CFB and HBB produced comparable results, but the ipsilateral lung yielded lesser amounts than the HBB. The decision score indicated a low performance level when using the TTM method, whereas the CBF method exhibited a slightly higher performance score than the HBB.
Findings: The CFB exhibited good performance in terms of the dose on OARs and at the matching fields. This method offers a comparable level of performance to the HBB. Thus, the CFB offers an alternative method of significant interest in PMRT.

Introduction

Breast cancer is the most commonly occurring form of cancer among women around the world.[1] Postmastectomy radiotherapy (PMRT) is recognised as an important form of treatment for advanced incidences of breast cancer. It can improve the chances of patients remaining disease-free and has been found to increase the overall survival rates of cancer patients.[2] Many current treatment techniques employ PMRT such as three-dimensional radiotherapy (3DRT),[3–7] ntensity-modulated radiotherapy[8,9] and volumetric arc radiotherapy.[10,11] Sophisticated techniques provide a high radiation dose to the target while preserving organs at risk (OARs); however, they require long periods of time for preparation and treatment.[12] In reality, the number of patients per treatment room is limited in contrast to the actual patient population. As has been previously mentioned with regard to sophisticated techniques, 3DRT is still a necessity in the treatment of this disease because of the short overall amount of treatment time involved and the low doses of radiation that are delivered to the OARs.[13,14]

3DRT is the basic technique employed to address this scourge. The three-fields technique, which consists of opposing tangential of the chest wall (CW) and anterior field of the supraclavicular (SC), is normally employed for the treatment planning. Various techniques are utilised such as the dual-isocenter technique (DIT), the single-isocenter technique (SIT) with various beam geometry methods. The DIT has been commonly used in the treatment planning. The problem associated with this method arises at the junction between opposing tangential fields (OTFs) and SC field (SCF). Consequently, the uncertainty associated with the setup process may impact the degree of dose homogeneity delivered at the junction.[15] Many methods have been proposed in an attempt to address this problem.[4–7] The SIT is just one of the techniques that has been proposed for effective treatment planning. SIT employing the half beam block (HBB) method[4,5] is one of the approaches used in the PMRT. Each half of the treatment field was utilised for the CW and SC; thus, the limitation of field size is transpired. The geometrical arrangement[6,7] is another approach for the dose homogeneity improvement. A formula is constructed to determine the angles of beam geometry, especially the couch rotation. A perfect dose

https://doi.org/10.1017/S1460396921000431 Published online by Cambridge University Press

homogeneity is found by utilising this approach. However, the degree of the uncertainty may raise by the rotating couch.

The immobilisation is one of the considerations in the PMRT. The Breast-board is the main device of various immobilisations. The disadvantages of this device are found not only a large setup error in the craniocaudal direction[16] but also an inconvenient and long setup time.[17] A Wing-board is the alternative device for immobilisation. The replacement of this device impacts the currently treatment method in our centre. Utilising this method with the Wing-board, a underdose is found at the junction between the two treatment fields.

Various methods have been proposed to solve the problem of field matching; however, there are various issues associated with the insufficient matching methods such as dose inhomogeneity at the junction, field size limitations and uncertainty of setup errors in the geometrical arrangements. This study, then, has proposed an alternative method of field matching that would improve dose homogeneity and minimise the limitations associated with the treatment field size. The proposed method uses the coplanar plane between the superior border of the medial tangential field and the inferior border of the SCF. To evaluate the performance of this approach, the SIT_{HBB} method was benchmarked with not only the proposed method but also the currently identified method (Traditional three-fields monoisocenter). The dosimetric comparison among the three methods has been analysed with the use of relevant statistics.

Materials and Methods

Ethical statement

In accordance with the requirements for prospective studies, the concept and study design of this study were submitted for ethical approval. Ethical clearance was granted by the Chiang Mai University Ethics Committee (study code: RAD-2563–07760).

Data preparation and sample size

All image sets of the patients were acquired by SOMATOM DefinitionAS (Siemens Healthineers, Germany) at 5 mm of slice thickness. A Wing-board (Standard Board™, CIVCO Radiotherapy, USA) was used for the immobilisation. Twenty-two patients of the left-side postmastectomy were randomly selected during the period of January 2019 to December 2020. The sample size was calculated according to the work of Naing et al.[18]

Treatment area and dose prescriptions

All plans were created with the use of the Pinnacle³ treatment planning system v.16.0 (Philips Radiation Oncology Systems, USA), and doses were delivered by Primus™ linear accelerator (Siemens Healthcare, Germany). The treatment area was specified according to Halperin *et. al.*[19] guideline. The medial, lateral, superior and inferior borders were drawn on the images of the CW and SC by radiation oncologists. The ipsilateral lung and heart were denealiated. LN I, II and III were delineated in order to evaluate the performance of various methods according to NRG Oncology.[20] The region of interest was created to investigate the dose at the junction area (so called '*ROIg*'). ROIg was constructed from the body surface on CT image at the junction between the tangential and SC fields including the adjacent upper and lower slices, as is shown in Figure 1. Doses (2·67Gy and 2·65Gy in 15 and 16 fractions, respectively) were prescribed at the isocentre/prescribed point on the CW and the prescribed point on the SC.

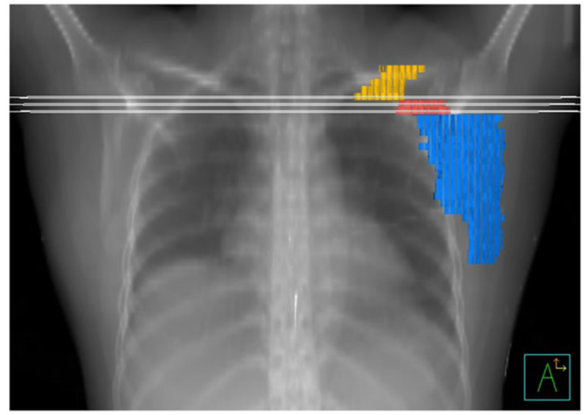

Figure 1. Region of interest at the matching area (ROIg) presents in the three white lines. Lymph node levels I, II and III are present in blue, red and yellow, respectively.

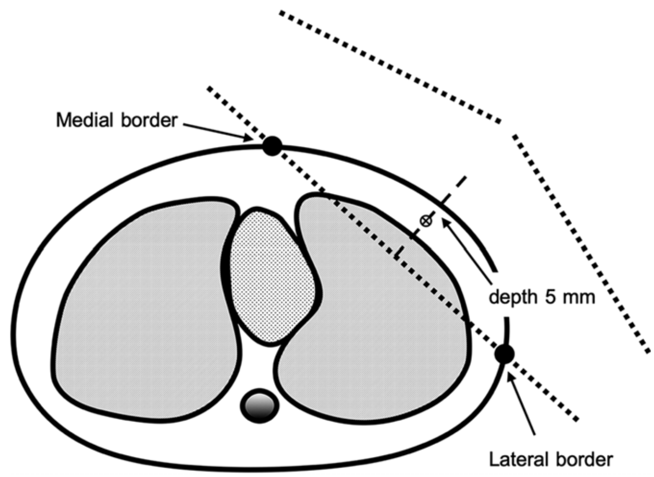

Figure 2. Diagram of the isocenter location of the opposing tangential fields.

Beam geometry methods

All plans employed the SIT, but beam arrangements were prepared differently. All three different methods were created on an image set of each patient and described as follows.

Coplanar field border (CFB) method

This proposed method was created to provide an alternative choice for PMRT. Accordingly, the slice at the centre between the superior and inferior border of the CW was selected. The isocenter was then placed on the perpendicular line of the midplane between the medial and lateral borders. This point was located 5 mm under the surface as is shown in Figure 2. The OTFs were then created. Instead of employing the parallel the chest curve, the collimator angle was determined as follow and demonstrated in Figure 3a:

$$\theta = 90 - \cos^{-1}\left(\frac{x}{100}\right) \quad (1)$$

where θ represents the collimator angle in the degree and x represents the upper half of the tangential field in centimeters. Figure 3d demonstrates the beam direction used in this method. Multi-leaf collimators blocked the lung at 2 cm from the rib cage. With this block, the partial heart was also blocked. The lateral tangential field

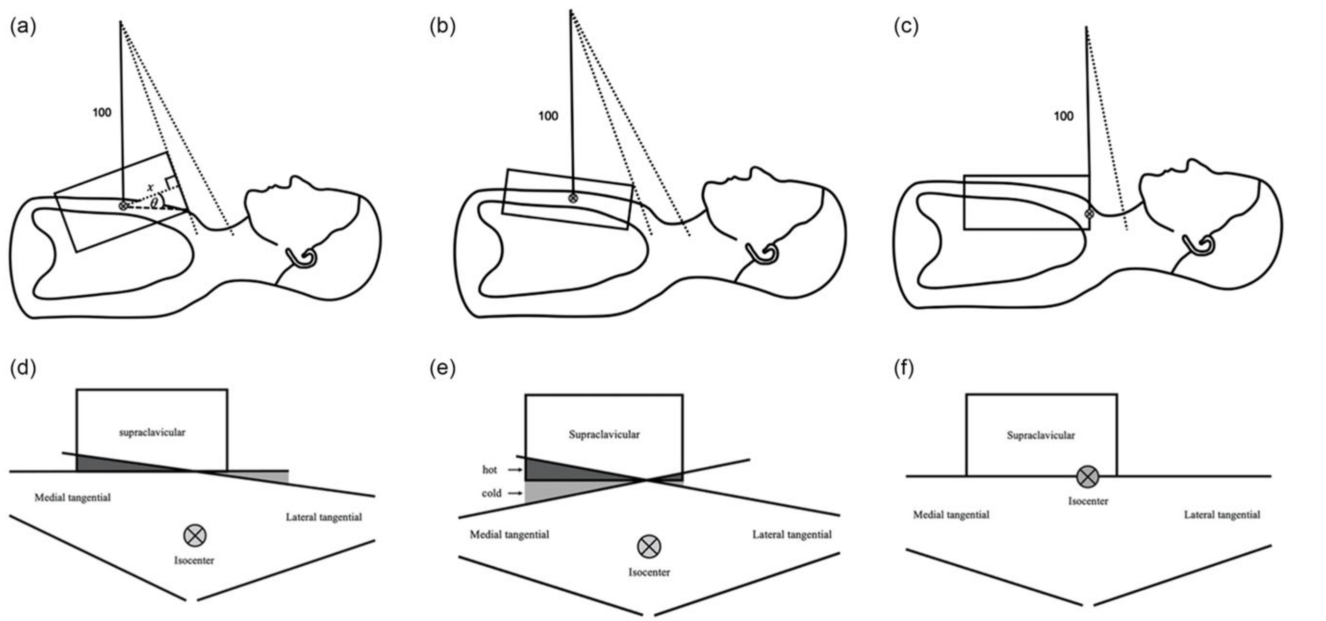

Figure 3. Diagram of various beam geometry method. top line shows the collimator direction, whereas the bottom line is the beam geometry. The CFB method demonstrates in (a) and (d). Figure (a) also shows the parameters for the calculation of the collimator angle (θ). The TTM method is in (b) and (e). Finally, the HBB method is in (c) and (f).

was created with the use of opposed beam geometry. The SCF was then prepared by sharing the isocenter with the OTFs. This field was limited by radiation oncologists. The inferior border of the SCF and the superior border of the OTFs were along the same line. The rectangular open field is normally used so as to exclude the head of the humerus. The prescribed point was neccesarilly used for this off-axis field. The point was placed on the slice of the mid-thoracic vertebral body level I. On this slice, this point was located 3 cm from the midline and at a depth of 3.5 cm from the surface on average. Figure 4a and 4b present an example of beam geometry of this method.

Traditional three-field monoisocenter (TTM) method

All patients had been previously treated with this method. The isocenter was placed at the same location as was used in the CFB method. The OTFs were then prepared as well. Collimators were used to rotate the treatment fields parallel to the chest curve, as is demonstrated in the Figure 3b. This tangential fields involved the lung no further than 2 cm at the isocenter plane. The SCF and the prescribed point were created by employing the same method used in the CFB. A diagram of this method is illustrated in Figure 3b and 3e. An example of the beam geometry is demonstrated in Figure 4c and 4d.

Half beam block (HBB) method

HBB is commonly used in conjunction with 3DRT in many treatment regions. The slice of the superior border of the CW was selected for this approach. The isocenter was placed in the same method used in the CFB. The lower half of the beam was used for the OTFs, whereas the upper half was used for the SC. The collimator angle was paralleled on the longitudinal axis. The lung and heart were blocked in the same way they were in the CFB. The SCF was also created in the same manner as was employed in the previous method. Figure 3c and f present a diagram of this method. Because the isocenter of this method was partially blocked, the prescribed point had to be created on the OTFs and the SCF. The prescribed points were placed at the same location as in the CFB. Accordingly, placements were designated at not only the isocenter of the OTFs but also at the prescribed point of the SCF. An example of this method is shown in Figure 4e and f.

To evaluate the performance among different methods, all beam angles of the three different approaches were fixed as were the radiation doses prescribed to the same points for all methods. The plan parameters of the patients are shown in Table 1. The maximum lung distance was the distance between the tangential field border and the rib cage. Beam separation was measured between the medial and lateral borders. The depth of the prescribed point on the SC was set and measured from the skin.

Plan evaluations

All treatment plans were accepted at 95% of the prescribed dose, whereas the dose coverage was evaluated by radiation oncologists. The acceptable criteria was based on the dose coverage and overdose volume. This dose coverage did not exceed the area of lung tissue by more than 2 cm from the rib cage. The dose of 2cc (D_{2cc}) also did not exceed 115% of the prescribed dose. The dosimetric parameters were evaluated on the ipsilateral lung and heart and investigated on LN I, II, II and ROIg. All levels of LNs were analysed on the mean dose (D_{mean}) and dose at 95% volume ($D_{95\%}$). The OARs were analysed on D_{mean}, percent volume at 5Gy (V_{5Gy}), 20Gy (V_{20Gy}) and 30Gy (V_{30Gy}) for the ipsilateral lung and D_{mean}, V_{10Gy} and V_{40Gy} for the heart. Furthermore, ROIg was analysed on $D_{2\%}$, D_{2cc} and D_{10cc}.

Statistical analysis

The results were analysed at 95% confidence intervals of the statistics. The Shapiro–Wilk test was used to evaluate the normal distribution of the dosimetric parameters. Repeated ANOVA test was used to evaluate the normal distribution of the results, whereas Friedmen's two-way ANOVA was used for the other group.

https://doi.org/10.1017/S1460396921000431 Published online by Cambridge University Press

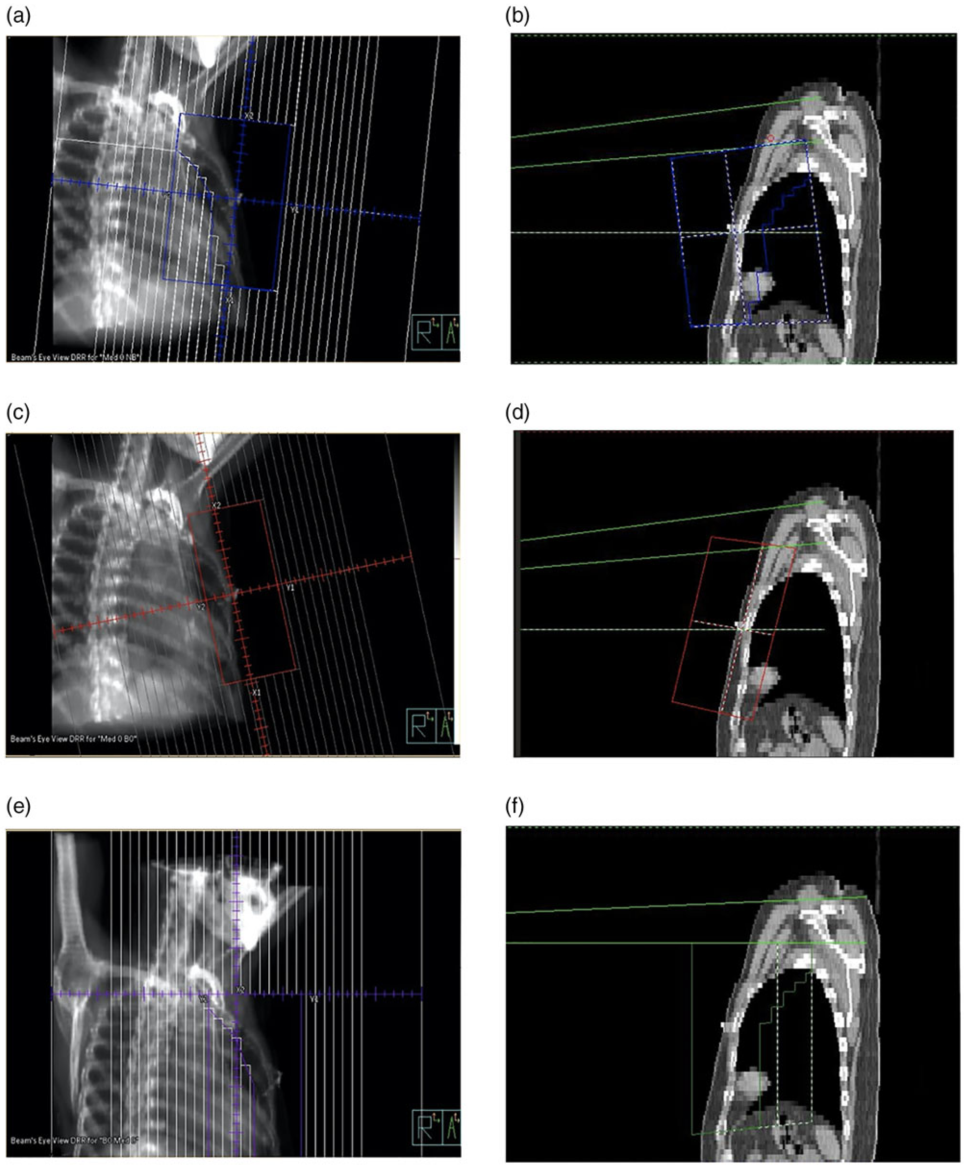

Figure 4. Demonstrates the example of three different methods in the 3DRT technique. (a) and (b) illustrate the CFB method. (a) shows the medial tangential field with the blocked lung, whereas Figure 4B demonstrates the off-axis SC field and the coplanar between the superior border of the medial tangential and inferior border of the SC field. (c) and (d) present the example of beam geometries by utilising the TTM method. The opposing tangential fields were placed on the chest wall as illustrated in (c). The off-axis SC field was created as shown in (d–f) present the beam geometries by using the HBB method. (e) reveals the medial tangential of the upper half beam block field. The beam uses the MLC for lung block. (f) demonstrates the SC field of the lower half beam block field.

Decision score

Decision score was used to evaluate the performance of each method. The score was considered based on the results that exhibited a significant difference when using the HBB benchmarks. Either plus one or minus one indicated that a result was either better or lesser, respectively, than the HBB method. No significant differences were observed between HBB and each of the other methods and, thus, they received no score.

Results

The test results indicate that V_{5Gy}, V_{20Gy} and D_{mean} values of LN I were of normal distribution, whereas the others revealed non-normal distribution. Table 2 presents the mean and standard deviation (Mean ± SD) values of the parameters when using various methods. The TTM method delivered significantly lower D_{mean} and V_{5Gy}, V_{20Gy} and V_{30Gy} values on the ipsilateral lung than the HBB method ($p = 0{\cdot}003$, $p = 0{\cdot}001$, $p = 0{\cdot}008$ and $p = 0{\cdot}002$, respectively). The CFB method presented a significantly higher V_{5Gy} value than the TTM ($p = 0{\cdot}001$), but a significantly lower V_{20Gy} value than the HBB method ($p = 0{\cdot}023$). The heart is one of the primary considerations when a lesion occurs in the left breast. The D_{mean} value of the heart revealed no significant differences among the three methods. The HBB method exhibited a significantly higher V_{10Gy} value on the heart than the TTM method ($p = 0{\cdot}007$). With regard to the V_{40Gy} value of the heart, the TTM method provided a significantly higher value than the CFB and HBB methods ($p < 0{\cdot}001$ and $p = 0{\cdot}008$, respectively). The LN coverage can present at the junction. The TTM method exhibited significantly lower D_{mean} and $D_{95\%}$ values on LNs I and II than both the CFB ($p \leq 0{\cdot}007$) and the HBB ($p \leq 0{\cdot}001$)

https://doi.org/10.1017/S1460396921000431 Published online by Cambridge University Press

Table 1. Treatment plan parameters

Parameter		Mean (range)
Prescribed dose (Gy)		41·8 (40·5 – 42·4)
Maximum lung distance (MLD: cm)		2·05 (1·31 – 3·11)
Beam separation (cm)		20·37 (15·12 – 35·21)
Prescribed depth of SC (cm)		3·66 (3·05 – 4·25)
Degree of gantry (degrees)	anterior SC field	0
	medial tangential field	303·71 (297·00 – 309·00)
	lateral tangential field	127·35 (120·00 – 133·00)

methods. LN III revealed parallel results to other LNs with the exception of D_{mean} ($p \leq 0{\cdot}006$). The $D_{95\%}$ value of LN III was found to be significantly higher when the HBB method was used rather than the CFB method ($p = 0{\cdot}001$). ROIg was created to determine the overdose/underdose specifications at the field junction The TTM method exhibited a significantly lower dose on ROIg than either the CFB ($p \leq 0{\cdot}001$) or the HBB ($p \leq 0{\cdot}003$) methods for all dosimetric parameters. However, the CFB method revealed a significantly higher D_{2cc} value on ROIg than the HBB method ($p = 0{\cdot}007$). Figure 5 illustrates the dose distribution and dose volume histogram of an example case with the use of the CFB, TTM and HBB methods.

Table 3 presents the significant difference parameters and decision scores of various methods by applying the HBB benchmark. The scores indicate only the significant differences between the methods. The D_{mean} value of the heart is the only parameter that indicated no significant differences among the various methods. The V_{20Gy} value of the ipsilateral lung when using the CFB method was also the only parameter that exhibited a significant difference when compared with the HBB method.

Discussion

The SIT with CFB method is an alternative beam geometry of our centre. The proposed method focused to improve the dose homogeneity at the junction. Performance was then evaluated using the dosimetric parameters on various levels of LN, OARs and ROIg. The TTM method is not widely used in many centres. The underdose was found at the junction by utilising these methods with Wing-board.

Various LN levels were not necessarily treated in the PMRT. These organs lie within the region of the matching fields that indicate dose homogeneity between the OTFs and SCF.[4,21] To ensure the evaluation of the overdose/underdose area only at the junction, ROIg was created. The results indicate slightly equivalent dose levels between $D_{2\%}$ and D_{10cc}. The CFB method focused on the coplanar plan only the medial tangential field. This proposed method would slightly increase the dose at the junction by the divergent of the lateral tangential field as is shown in Figure 3e. This overdose was increased to 106·6%, 115·1% and 107·3% of the mean prescribed dose for $D_{2\%}$, D_{2cc} and D_{10cc}, respectively.

By using the SIT without HBB method, the outcomes of this study were almost inline with the study of Zhang et al.[7] However, hybrid planning was utilised in their work but not for this study. A perfect dose homogeneity was revealed in their research when the rotations of the couch were required. The couch rotation was unnecessarily used in this proposed method resulting in a high dose on the medial border of the SCF; however, the overdose volume was determined to be acceptable.

The decision score clearly showed that the OARs of the TTM method received a lower dose than the others. However, this method also revealed a low dose by the observation of the LNs. The CFB method exhibited a good level of performance, but the D_{2cc} value of the ROIg received a significantly higher dose than in the HBB method ($p = 0{\cdot}007$). The ROIg was not included in

Table 2. Mean and standard deviation (Mean ± SD) of dosimetric parameters by using various beam geometries

Structure	TTM	CFB	HBB	*p*-value
Ipsilateral Lung				
D_{mean} (Gy)	10·00 ± 8·13	10·46 ± 7·48	10·87 ± 7·63	b ($p = 0{\cdot}003$)
V_{5Gy} (%)	29·23 ± 7·63	32·91 ± 6·60	34·23 ± 7·28	a ($p < 0{\cdot}001$)
				b ($p < 0{\cdot}001$)
V_{20Gy} (%)	15·59 ± 5·19	17·95 ± 5·14	19·27 ± 5·75	b ($p = 0{\cdot}008$)
				c ($p = 0{\cdot}023$)
V_{30Gy} (%)	12·09 ± 4·46	12·95 ± 4·33	13·86 ± 5·13	b ($p = 0{\cdot}002$)
Heart				
D_{mean} (Gy)	3·91 ± 1·37	4·06 ± 0·82	4·06 ± 0·78	–
V_{10Gy} (%)	7·77 ± 3·78	8·41 ± 2·50	8·86 ± 2·46	b ($p = 0{\cdot}007$)
V_{40Gy} (%)	2·45 ± 1·65	1·23 ± 1·02	1·14 ± 1·25	a ($p < 0{\cdot}001$)
				b ($p = 0{\cdot}008$)
Lymph node				
- Level I				
D_{mean} (Gy)	27·48 ± 7·44	31·82 ± 6·92	31·91 ± 7·25	a ($p = 0{\cdot}007$)
				b ($p < 0{\cdot}001$)
$D_{95\%}$ (Gy)	5·24 ± 6·12	8·48 ± 8·73	7·76 ± 8·89	a ($p < 0{\cdot}001$)
				b ($p < 0{\cdot}001$)
- Level II				
D_{mean} (Gy)	26·79 ± 8·05	37·21 ± 6·79	39·73 ± 2·74	a ($p < 0{\cdot}001$)
				b ($p < 0{\cdot}001$)
$D_{95\%}$ (Gy)	14·31 ± 10·56	29·28 ± 7·71	33·09 ± 7·01	a ($p < 0{\cdot}001$)
				b ($p < 0{\cdot}001$)
- Level III				
D_{mean} (Gy)	39·33 ± 4·45	41·35 ± 2·25	41·65 ± 2·20	a ($p = 0{\cdot}006$)
				b ($p = 0{\cdot}002$)
$D_{95\%}$ (Gy)	35·52 ± 10·99	35·71 ± 7·12	37·95 ± 4·21	b ($p < 0{\cdot}001$)
ROIg				
$D_{2\%}$ (Gy)	39·83 ± 3·34	44·58 ± 1·95	44·14 ± 1·83	a ($p < 0{\cdot}001$)
				b ($p < 0{\cdot}001$)
D_{2cc} (Gy)	44·27 ± 3·27	48·10 ± 2·30	46·70 ± 1·84	a ($p < 0{\cdot}001$)
				b ($p = 0{\cdot}003$)
				c ($p = 0{\cdot}007$)
D_{10cc} (Gy)	39·94 ± 4·93	44·86 ± 2·47	44·34 ± 1·94	a ($p < 0{\cdot}001$)
				b ($p < 0{\cdot}001$)

*a is TTM versus CFB methods, b is TTM versus HBB methods and c is CFB versus HBB methods.

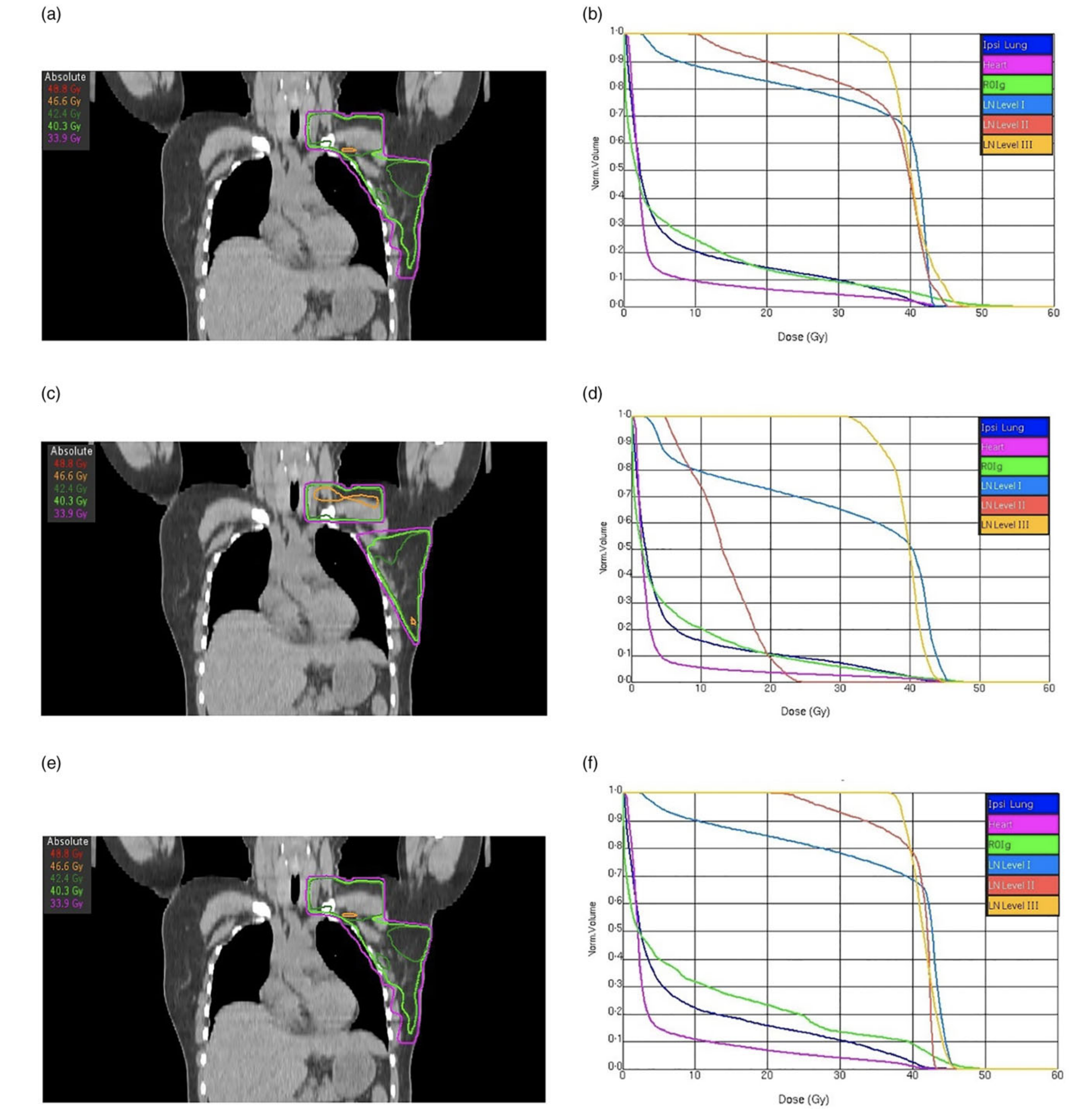

Figure 5. Dose distribution and dose volume histogram (DVH) of the example case by utilising three different methods. Left column is the dose distribution where the evaluated dose presents in light green line (40·3 Gy). Right column is the histogram between the proportion of normalised organ volume versus the absolute dose in Gy. Top, middle and bottom are the example results by employing the CFB, TTM and HBB, respectively.

the decision score because the HBB method also provided a high dose at the junction (D_{2cc} = 111·7% of the mean prescribed dose). The degree of dose homogeneity in the large volume, however, revealed no significant differences between the CFB and HBB methods.

The CFB method provided a full range of field size for the CW and improved dose homogeneity at the junction. The degree of dose homogeneity was not as optimal as the HBB method, but the volume of overdose was acceptable. The ipsilateral lung of the CFB method received a lower dose than with the HBB method because of the beam divergence. The off-axis SCF from the CFB method projected obliquely up to the apex of the lung as is shown in Figure 6. As a consequence of the rotation of the collimator, the dose was fulfilled at the junction when using the CFB method, but not when using the TTM method. The proposed method increased the dose on OARs when compared with the TTM method, but these outcomes were determined to be acceptable. The proposed method, however, provided an advantage for the matching fields, but this is related to the accuracy of the treatment unit as all beam patterns. Thus, the uncertainty of the relevant mechanics requires

Table 3. Mean and standard deviation (Mean ± SD) of the dosimetric parameters using HBB benchmark, including the decision score

Structure	Mean ± SD HBB	Mean ± SD TTM	Mean ± SD CFB	Decision Score TTM	Decision Score CFB
Ipsilateral Lung					
D_{mean} (Gy)	10·87 ± 7·63	10·00 ± 8·13 $p = 0{\cdot}003$	–	1	0
V_{5Gy} (%)	34·23 ± 7·28	29·23 ± 7·63 $p < 0{\cdot}001$	–	1	0
V_{20Gy} (%)	19·27 ± 5·75	15·59 ± 5·19 $p = 0{\cdot}008$	17·95 ± 5·14 $p = 0{\cdot}023$	1	1
V_{30Gy} (%)	13·86 ± 5·13	12·09 ± 4·46 $p = 0{\cdot}002$	–	1	0
Heart					
D_{mean} (Gy)	–	–	–	0	0
V_{10Gy} (%)	8·86 ± 2·46	7·77 ± 3·78 $p = 0{\cdot}007$	–	1	0
V_{40Gy} (%)	1·14 ± 1·25	2·45 ± 1·65 $p = 0{\cdot}008$	–	−1	0
Lymph node					
- Level I					
D_{mean} (Gy)	31·91 ± 7·25	27·48 ± 7·44 $p < 0{\cdot}001$	–	−1	0
$D_{95\%}$ (Gy)	7·76 ± 8·89	5·24 ± 6·12 $p < 0{\cdot}001$	–	−1	0
- Level II					
D_{mean} (Gy)	39·73 ± 2·74	26·79 ± 8·05 $p < 0{\cdot}001$	–	−1	0
$D_{95\%}$ (Gy)	33·09 ± 7·01	14·31 ± 10·56 $p < 0{\cdot}001$	–	−1	0
- Level III					
D_{mean} (Gy)	41·65 ± 2·20	39·33 ± 4·45 $p = 0{\cdot}002$	–	−1	0
$D_{95\%}$ (Gy)	37·95 ± 4·21	35·52 ± 10·99 $p < 0{\cdot}001$	–	−1	0
Total score				−2	1

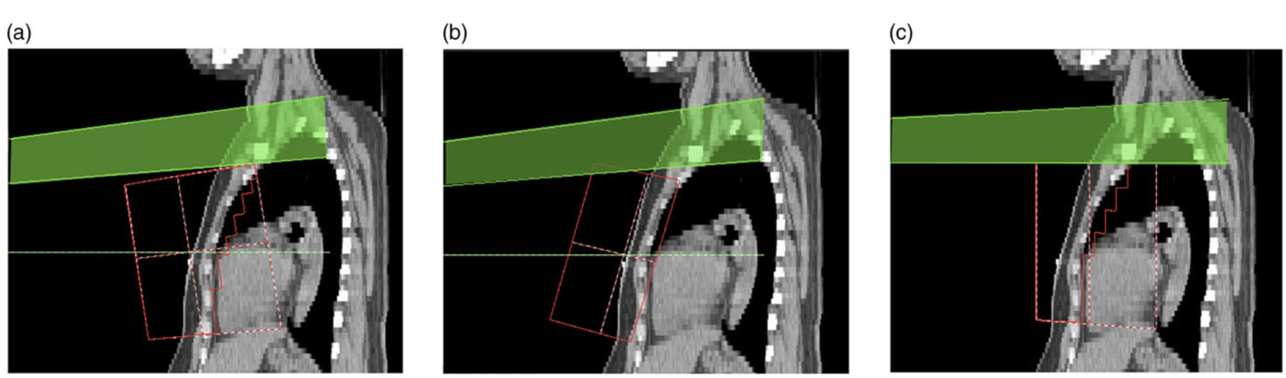

Figure 6. Impact of SC field direction by utilising three different method. The off-axis beam shows the divergence out of the lung apex on the CFB (a) and TTM (b) methods, whereas no divergence at the central beam is on the HBB (c) method.

https://doi.org/10.1017/S1460396921000431 Published online by Cambridge University Press

further investigation. The clinical outcome is one of the consideration issues. The skin reaction at the junction and the tumor recurrence required an exploration.

Conclusion

PMRT has recently required 3DRT. The number of patients and treatment times were most impacted when sophisticated techniques were used. This study has proposed a alternative beam geometry for PMRT. Consequently, the CFB method improved the degree of dose homogeneity at the junction between the tangential and SC fields, whereas the dose delivered to OARs remained low. This method was found to not only produce comparable results but also minimised the limitations of the HBB method.

Conflict of Interest. None.

References

1. Sung H, Ferlay J, Siegel RL et al. Global cancer statistics 2020: GLOBOCAN estimates of incidence and mortality worldwide for 36 cancers in 185 countries. CA Cancer J Clin 2021. https://doi.org/10.3322/caac.21660
2. Recht A, Edge SB, Solin LJ et al. Postmastectomy radiotherapy: clinical practice guidelines of the American Society of Clinical Oncology. J Clin Oncol 2001; 19 (5): 1539–1569. https://doi.org/10.1200/JCO.2001.19.5.1539
3. Yousefi Kashi AS, Karimi M, Rakhsha A, Javadzadegan A, Taghizadeh-Hesary F. The Troponin-I release in patients with left-sided early-stage breast cancer undergoing adjuvant whole breast radiotherapy: an Iranian experience. Int J Cancer Manage 2020; 13 (10). https://doi.org/10.5812/ijcm.107043
4. Banaei A, Hashemi B, Bakhshandeh M. Comparing the monoisocentric and dual isocentric techniques in chest wall radiotherapy of mastectomy patients. J Appl Clin Med Phys 2015; 16 (1): 130–138. https://doi.org/10.1120/jacmp.v16i1.5069
5. Wadasadawala T, Lewis S, Gaikwad U et al. Mono versus dual isocentric technique for breast cancer radiotherapy: evaluation of planning, dosimetry and treatment delivery. J Radiother Pract 2020: 1–6. https://doi.org/10.1017/S1460396920000667
6. Romeo N. A new isocentric technique for exact geometric matching in the radiotherapy of the breast and ipsilateral supraclavicular fossa using dual asymmetric jaws. Phys Med 2012; 28 (4): 281–287. https://doi.org/10.1016/j.ejmp.2011.10.003
7. Zhang T, Dilworth JT, Marina O, Chen P, Benedetti L, Liu Q. A three-field monoisocentric inverse breast treatment planning technique without half-beam blocking. J Appl Clin Med Phys 2015; 16 (5): 246–258. https://doi.org/10.1120/jacmp.v16i5.5494
8. Wang Q, Jie W, Liang Z, Wu H, Cheng J. Postmastectomy intensity modulation radiated therapy of chest wall and regional nodes: Retrospective analysis of the performance and complications up for 5 years. Medicine 2017; 96 (39). https://doi.org/10.1097/MD.0000000000007956
9. Koshy M, Zhang B, Naqvi S, Liu B, Mohiuddin MM. A novel technique for post-mastectomy breast irradiation utilising non-coplanar intensity-modulated radiation therapy. B J Radiol 2010; 83 (994): 874–881. https://doi.org/10.1259/bjr/59469015
10. Iorio GC, Franco P, Gallio E, et al. Volumetric modulated arc therapy (VMAT) to deliver nodal irradiation in breast cancer patients. Med Oncol 2018; 35 (1): 1–8. https://doi.org/10.1007/s12032-017-1061-8
11. Nichols GP, Fontenot JD, Gibbons JP, Sanders ME. Evaluation of volumetric modulated arc therapy for postmastectomy treatment. Radiat Oncol 2014; 9 (1): 1–8. https://doi.org/10.1186/1748-717X-9-66
12. Foroudi F, Wilson L, Bressel M, et al. A dosimetric comparison of 3D conformal vs intensity modulated vs volumetric arc radiation therapy for muscle invasive bladder cancer. Radiat Oncol 2012; 7 (1): 1–0.
13. Liu H, Chen X, He Z, Li J. Evaluation of 3D-CRT, IMRT and VMAT radiotherapy plans for left breast cancer based on clinical dosimetric study. Comput Med Imaging Graph 2016; 54: 1–5. https://doi.org/10.1016/j.compmedimag.2016.10.001
14. Haertl PM, Pohl F, Weidner K, Groeger C, Koelbl O, Dobler B. Treatment of left sided breast cancer for a patient with funnel chest: volumetric-modulated arc therapy vs. 3D-CRT and intensity-modulated radiotherapy. Med Dosim 2013; 38 (1): 1–4. https://doi.org/10.1016/j.meddos.2012.04.003
15. Mahmoud A, Somayeh N, Mahbod E, Mehdi A, Vahid C, Ghazale G. Optimization of three dimensional planning dosimetric in breast phantom for match region of supraclavicular and tangential fields. J Cancer Res Ther 2013; 9 (1): 64. https://doi.org/10.4103/0973-1482.110376
16. Nalder CA, Bidmead AM, Mubata CD, Tait D, Beardmore C. Influence of a vac-fix immobilization device on the accuracy of patient positioning during routine breast radiotherapy. Br J Radiol 2001; 74 (879): 249–254. https://doi.org/10.1259/bjr.74.879.740249
17. Raza W, Agarwal S, Das KJ, Kumar SK, Lal P. Comparison of set-up errors by breast size on wing board by portal imaging. Rep Pract Oncol Radiother 2016; 21 (5): 447–452. https://doi.org/10.1016/j.rpor.2016.04.001
18. Naing L, Winn T, Rusli BN. Practical issues in calculating the sample size for prevalence studies. Arch Orofacial Sci 2006; 1: 9–14.
19. Halperin E, Perez C, Brady L, editors. Perez and Brady's Principles and Practice of Radiation Oncology, 5th edition. Philadelphia: A WALTER KLUWER business: c2008. Chapter 53: Early stage Breast Cancer; pp. 1175–1292.
20. NRG Oncology. Breast Cancer Atlases, Templates, & Tools. [Internet]. Philadephia: NRG oncology; 2019 [Cited 1 July 2019]. Available from: http://www.nrgoncology.org/Portals/0/Scientific%20Program/CIRO/Atlases/BreastCancerAtlas_corr.pdf?ver=2018-04-18-144201-270
21. Nadi S, Abedi-Firouzjah R, Banaei A, Bijari S, Elahi M. Dosimetric comparison of level II lymph nodes between mono-isocentric and dual-isocentric approaches in 3D-CRT and IMRT techniques in breast radiotherapy of mastectomy patients. J Radiother Pract 2020; 19 (3): 254–258. https://doi.org/10.1017/S146039691900061X